DESIGN OF AN ANTILOCK BRAKING SYSTEM CONTROLLER

J. O. Pedro [*,1] **O. T. Nyandoro** [**] **C. G. Bigg** [*]
K. Gross [*] **J. T. Nelson** [*]

[*] *School of Mechanical, Industrial and Aeronautical Engineering*
[**] *School of Electrical and Information Engineering, University of the Witwatersrand, Johannesburg.*

Abstract: The design of an antilock braking system controller (ABS), that automatically minimizes the braking distance by adjusting the braking torque in response to the wheel slip, is developed and experimentally tested for a quarter-car model. A robust, real-time proportional-plus-integral (PI) controller algorithm for the wheel slip is implemented through a microcontroller GPC850. The controller gains are scheduled based on the rotational velocity of the driving wheel.

Keywords: ABS, PI controller, nonlinear control system, wheel slip.

1. INTRODUCTION

The world's first ABS controller for passenger cars was introduced in 1978 by Bosch, with the primary objectives of preventing wheel-lock, reducing stopping distance, and enhancing steerability during braking (Johansen *et al.*, 2003), (Petersen *et al.*, 2003), (Will *et al.*, 1998), and (Solyom, 2002). There are conceptually two types of control strategies being used in ABS controllers: (a) acceleration-control based, and (b) slip-control based. The former indirectly controls the slip by using wheel deceleration/acceleration which is computed from the wheel angular velocity measurements. The major disadvantage of this method of control are the noticeable vibrations experienced during braking. Theoretically, the slip-control based method is the ideal method. It involves keeping the actual slip rate at an optimal target slip using continuous control during braking (Jun, 1998).

Various researchers have suggested different control approaches for designing the ABS controller. Most of the current mass production ABS controllers are rule based (Wellstead and Pettit, 1997). (Solyom, 2002) uses PI and PID control with gain scheduling based on the vehicle speed. (Jiang and Gao, 2001) show that nonlinear PID controller achieves better braking performance than conventional PID controller and loop-shaping controller. Sliding mode-type approaches to slip control are considered in (Buckholtz, 2002), (Will *et al.*, 1998), and (Drakunov *et al.*, 1995). LQR approaches with gain scheduling based on vehicle speed are used in (Johansen *et al.*, 2003), (Petersen *et al.*, 2003), and (Johansen *et al.*, 2001) to design ABS controllers.

This paper focusses on extending and implementing the ABS schemes proposed mainly by (Schinkel, n.d.) and (Solyom, 2002) for a special class braking systems actuated by fast acting electromechanical systems. A further contribution is the use of a resource constrained general purpose microcontroller as oppposed to the use of a onboard microcomputer as is most implementations.

[1] All correspondence should be addressed to this author, Email: jpedro@mech.wits.ac.za, Tel: 011 717 7317

The paper is outlined as follows. Section 2 gives the system description together with the mathematical model of a quarter-car. Stability analysis of the plant is carried out in this section by casting the system nonlinear equations into piecewise linear equations. ABS Controller design is presented in section 3. The PI controller gains are tuned for best braking performance in this section. Section 4 presents the numerical simulation of the plant with the controller in Simulink. The paper closes with conclusions and recommendations for future works.

2. SYSTEM MODEL

The system is a combination of an Atmel General Purpose microcontroller (AT90S8535) microcontroller, which is programmable using BASCOM-AVR, an electromagnetic braking mechanism and an appropriate power supply and amplifier to amplify the signal from the controller. The integrated system representation is indicated in Fig. 1. The braking mechanism consists of the following: an optical encoder, a small driven wheel, a brake disk, and a brass shaft that holds the components together. The proposed braking mechanism employed in the model validation system uses a mild steel casing to neatly encase the coil and acts as a journal bearing for the brass shaft. The casing has a steel core situated at its centre; the core is used as an electromagnet, and is energized by the coil. Once the coil is energized it sets up magnetic fields within the core, which attracts the brake disk, the disk then clamps against the outer rim of the casing causing a substantial amount of friction, and this in turn creates the retarding torque. The braking mechanism is coupled to a larger driving wheel, to simulate the effect of a driven wheel translating on a stationary surface. Fig. 2 shows the complete mechanical system.

Applying Newton's law to the quarter-car model shown in Fig. 3 gives the equations of motion as follows:

$$I_{dr}\dot{\omega}_{dr} = -\mu\left(\lambda\left(t\right)\right)NR_{dr}$$
$$I_w\dot{\omega}_w = R_w\mu\left(\lambda\left(t\right)\right)N - M_{br} \quad (1)$$

where I_{dr} and I_w are the moments of inertia of the driving and driven wheels respectively, ω_{dr} and ω_w are the angular velocities of the driving and driven wheels respectively, R_{dr} and R_w are the radii of the driving and driven wheels respectively, N is the interface normal force, M_{br} is the braking torque, μ is the interface friction coefficient, and λ is the longitudinal wheel slip. The wheel slip is defined as:

$$\lambda = 1 - \frac{R_w\omega_w}{R_{dr}\omega_{dr}} \quad (2)$$

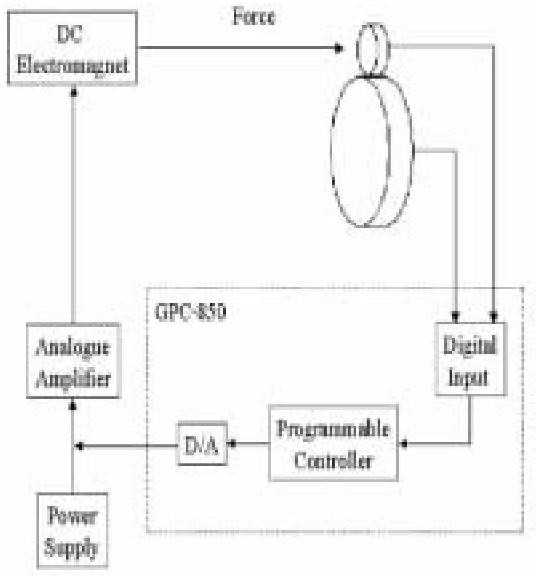

Fig. 1. System block diagram

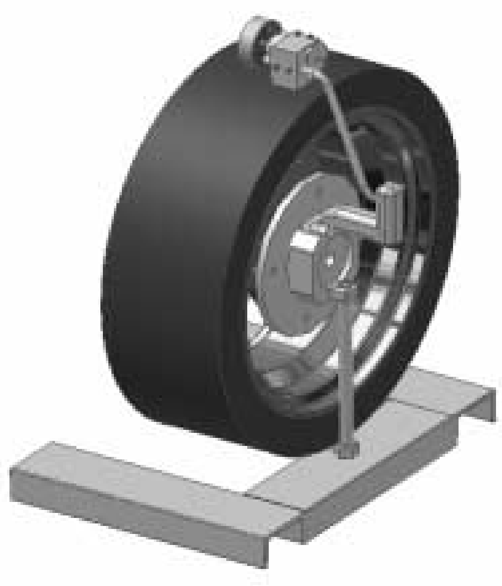

Fig. 2. Complete mechanical system

Hence, a locked wheel ($\omega_w = 0$) is described by $\lambda = 1$, while the free motion of the wheel is described by $\lambda = 0$. The interface coefficient of friction, μ, depends nonlinearly on the longitudinal wheel slip. Typical plots of friction coefficients versus longitudinal wheel slip for different surface conditions are shown in Fig. 4. Using (1) and (2) for $\omega_{dr} > 0$ and $\omega_w \geq 0$ gives the wheel slip dynamics:

$$\dot{\lambda} = -\frac{\mu(\lambda)N}{\omega_{dr}}\left[\frac{1}{I_{dr}}\left(1-\lambda\right) + \frac{R_w^2}{I_wR_{dr}}\right] + \frac{M_{br}}{I_wR_{dr}\omega_{dr}} \quad (3)$$

$$I_{dr}\dot{\omega}_{dr} = -\mu\left(\lambda\right)NR_{dr} \quad (4)$$

When ω_v tends to zero, the dynamics of the open loop system becomes infinitely fast with infinite gain (Johansen *et al.*, 2003).

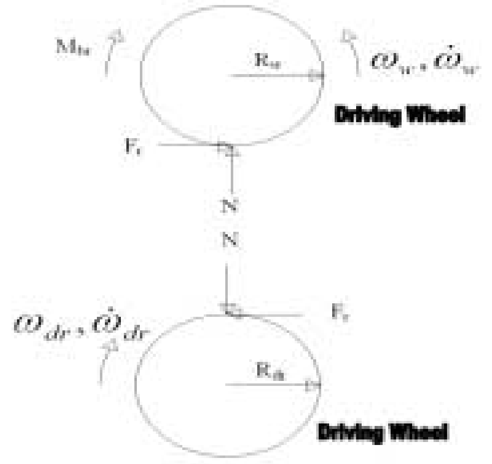

Fig. 3. Free-body diagrams of the driving and

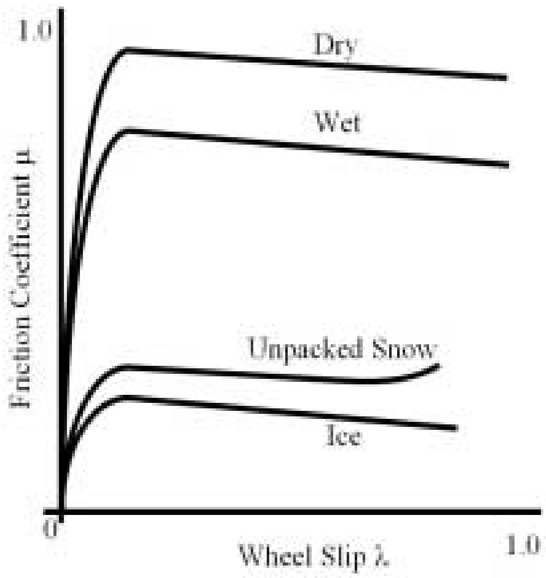

Fig. 4. Typical friction coefficient curves for different surface conditions

Assuming that the rotational velocity of the drum varies more slowly than other variables and letting $A = R_w/(I_w R_{dr})$ gives:

$$\dot{\lambda}\omega_{dr} = -\mu N R_w A + M_{br} A \tag{5}$$

Letting $\beta = NR_w A$, one obtains the final expression of the single-input-single-output control problem

$$\dot{\lambda} = \frac{\beta}{\omega_{dr}} - \mu\left(\lambda\left(t\right)\right) + \frac{A}{\omega_{dr}} M_{br} \tag{6}$$

The task of the ABS controller is to robustly stabilize the system around the maximum friction, such that a minimum braking time is needed and the car's steerability is maintained. In order to analyze the stability of the system and design the controller, it is necessary to cast the nonlinear equations into piecewise linear equations. This may be done by approximating the friction/slip curves by piecewise linear functions. After a piecewise linear representation for the friction/slip curves has been found the nonlinear model of the braking quarter car may be linearized. In order to cover all possible dynamics, it is appropriate to approximate the $\mu(\lambda)$ curves with two piecewise linear functions:

$$\begin{aligned} \mu &= a\lambda \quad \text{for} \lambda \leq 0.1 \\ \mu &= -\frac{1}{4}\lambda + \frac{3}{4} \pm 0.2 \quad \text{for} \lambda > 0.1 \end{aligned} \tag{7}$$

where a ∈ [5.75; 9.75] and the notation ±0,2 indicates that any arbitrary, not necessarily fixed, value can be assumed in the interval (-0.2, 0.2). With this approximation one may cover most values of μ.

For linearization one may approximate the system by the first terms of the Taylor series:

$$\begin{aligned} f\left(\lambda, \omega_{dr}\right) \approx f\left(\lambda_0, \omega_{dr_0}\right) + \left(\frac{\partial f}{\partial \lambda}\right)_{\lambda_0, \omega_{dr_0}} \left(\lambda - \lambda_0\right) \\ + \left(\frac{\partial f}{\partial \omega_{dr}}\right)_{\lambda_0, \omega_{dr_0}} \left(\omega - \omega_{dr_0}\right) \end{aligned} \tag{8}$$

such that one will get a linear (affine) system description:

$$\begin{aligned} \dot{x} &= A_q x + B u^* + E_q \\ y &= C_q x \\ q &= f\left(x\right) \end{aligned} \tag{9}$$

where x and q are the continuous and discrete states respectively. The term u(t) is the control input and A_q, B and C_q are the system, input and output matrices, respectively, of the subsystems. E_q are the affine terms and f(x) is the function indicating which subsystem is valid. For each subsystem q ∈ [1, 2, . . ., M], which are subsystems where $\lambda \leq 0.1$ one obtains:

$$A_q = \begin{bmatrix} 0 & -\frac{aNR_{dr}}{I_{dr}} \\ a\frac{\beta\lambda_0}{\omega_{dr_0}^2} & -a\frac{\beta}{\omega_{dr_0}} \end{bmatrix} \tag{10}$$

$$E_q = \begin{bmatrix} 0 \\ -a\frac{\beta\lambda_0}{\omega_{dr_0}} \end{bmatrix} \tag{11}$$

and for subsystems q ∈ [M+1, M+2,,N], which are subsystems where $\lambda > 0.1$ one obtains:

$$A_q = \begin{bmatrix} 0 & \frac{NR_{dr}}{4I_{dr}} \\ \frac{\beta}{\omega_{dr_0}^2}\left(\left(-\frac{1}{4}\lambda_0 + \frac{3}{4}\right) \pm 0.2\right) & \frac{\beta}{4\omega_{dr_0}} \end{bmatrix} \tag{12}$$

$$E_q = \begin{bmatrix} \left(-\frac{3}{4} \pm 0.2\right) \frac{NR_{dr}}{I_{dr}} \\ \frac{\beta}{\omega_{dr_{wp}}} \left(\left(\frac{1}{2}\lambda_{wp} - \frac{3}{2}\right) \pm 0.4\right) \end{bmatrix} \quad (13)$$

and $B^T = [0, A]$, $u^* = u \cdot \omega_{dr}$ and $x^T = [\omega_{dr}, \lambda]$ for q ∈ [1, 2, …, N]. It may be seen that the time-varying nonlinear system has been cast into a linear hybrid system with uncertainty.

For the stability analysis the system matrices are transformed into controller canonical form: $\overline{A_q} = TA_qT^{-1}$ with T_1 and T_2:

$$T_1 = \begin{bmatrix} -\frac{I_{dr}}{aNR_{dr}} & 0 \\ 0 & 1 \end{bmatrix} \quad T_2 = \begin{bmatrix} \frac{4I_{dr}}{NR_{dr}} & 0 \\ 0 & 1 \end{bmatrix} \quad (14)$$

such that where $\lambda \leq 0.1$:

$$\overline{A_q} = \begin{bmatrix} 0 & 1 \\ -a^2 \frac{\beta\lambda_0 I_{dr}}{NR_{dr}\omega_{dr_0}^2} & -a\frac{\beta}{\omega_{dr_0}} \end{bmatrix} \quad (15)$$

and where $\lambda > 0.1$:

$$\overline{A_q} = \begin{bmatrix} 0 & 1 \\ \frac{NR_{dr}\beta}{4I_{dr}\omega_{dr_0}^2} \left(\left(-\frac{1}{4}\lambda_0 + \frac{3}{4}\right) \pm 0.2\right) & \frac{\beta}{4\omega_{dr_0}} \end{bmatrix} \quad (16$$

Since the system matrices are now given in controller canonical form it is possible to inspect whether or not the systems are stable. A system is Hurwitz stable if and only if all coefficients in the lowest row of the system matrix in controller canonical form are negative. One may immediately see that the subsystems q ∈ [1, 2,…, M], i.e., subsystems where $\lambda \leq 0.1$ are stable since the coefficients in the lower row of the system matrices are negative for all possible parameter variations. However, the subsystems q ∈ [M+1, M+2, …, N], i.e., systems where $\lambda > 0.1$, are not globally stable. None of the subsystems are valid on the whole state space, however, and hence a check must be performed to ascertain if the subsystems for $\lambda > 0.1$ converge for $0.1 < \lambda \leq 1$ and $0 < \omega_{dr}$. Taking equation 1 and applying equation 9 for $\lambda > 0.1$

$$\dot{\omega}_{dr} = \frac{R_{dr}N\lambda}{4I_{dr}} + \left(-\frac{3}{4} \pm 0.2\right) \frac{R_{dr}N}{I_{dr}} \quad (17)$$

which is less than zero for all values of slip, λ, in the constraint as the maximum is seen to be when $\lambda = 1$, which is negative. Hence for all values of λ and ω_{dr} the differential equation converges to values which belong to subsystems represented in system (12). The differential equation for λ in the region $\lambda > 0.1$:

$$\dot{\lambda} = \frac{\beta\lambda}{4\omega_{dr}} + \left(-\frac{3}{4} \pm 0.2\right) \frac{\beta}{\omega_{dr}} \quad (18)$$

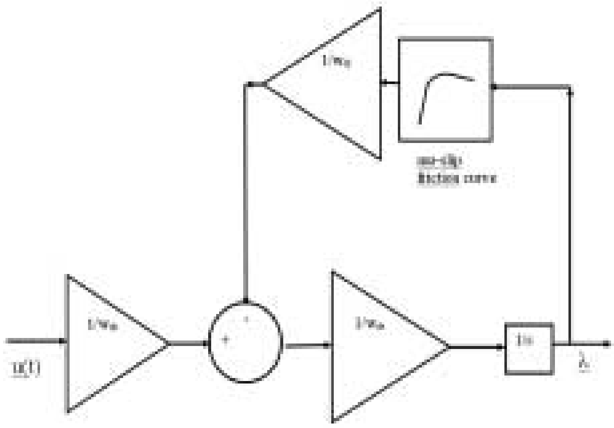

Fig. 5. Control problem system diagram.

has a right hand-side which is also negative for all admissible λ and ω_{dr}. This can be seen if a value of λ is substituted which would make the equation as least negative as possible. This value is $\lambda = 1$, which indicates that the equation is negative for all admissible velocities ω_{dr}. Hence, this differential equation also converges to values of λ which belong to subsystems (12), for all admissible values of the states. It was illustrated that the subsystems (12) and (14) converge individually, for all admissible initial states, to $x = 0$. In general this does not mean that the whole system is stable. However, since the states converge for any initial condition from subsystems (14) to states which belong to the subsystems (12) and (12) converges to zero, $x \to 0$ as $t \to \infty$ and hence the system is stable.

3. CONTROLLER DESIGN

The system diagram corresponding to the statement of the control problem presented in equation 5 is illustrated in figure 5 where the input to the system u(t) is the braking torque. Due to high uncertainty in the real process, it is natural to look for a simple robust controller which can easily be tuned. Therefore, a PI (proportional-integral) controller was selected and the gains are scheduled based on the rotational velocity of the driving wheel. The bandwidth of this model may be shown to be directly related to ω_{dr}, that is, the bandwidth is smaller for higher ω_{dr}. Therefore, it is natural to design the controller to counteract this variation. The controller gains are scaled by ω_{dr} to ensure a higher gain for high rotational velocities. In particular, when the system is operating at maximum friction, i.e., at the top of the friction curve, this scaling will theoretically remove the dependence on velocity of the driving wheel.

The objective is to design a controller which decelerates the vehicle as fast as possible and maintains steerability. From previous analysis, the maximum deceleration is reached at a slip of $\lambda =$ 0,1.

At such a slip the wheel is far from being locked, which implies that the steerability of the car may be maintained. We have also seen that it is sensible to approximate the nonlinear car dynamics by equations 12 and 14. For equation 12, i.e. subsystems where $\lambda \leq 0.1$, the primary objective would be to increase or maintain λ such that $\dot{\lambda} \geq 0$. For equation 14 λ is required to be reduced such that one may obtain better steerability and braking performance, i.e. we would like $\dot{\lambda} < 0$. We compute now the control input space in dependence of the state space. For $\dot{\lambda} \leq 0$:

$$0 \leq -\frac{\beta}{\omega_{dr}} a\lambda + \frac{A}{\omega_{dr}} M_{br} \tag{19}$$

and hence

$$\frac{\beta}{A} a\lambda \leq M_{br} \tag{20}$$

Similarly, for the condition of $\lambda > 0.1$:

$$\frac{\beta}{A}\left(-\frac{1}{4}\lambda + \frac{3}{4} \pm 0.2\right) \geq M_{br} \tag{21}$$

Hence, limits on the braking torque have been generated which will ensure that wheel lock will not occur for the system on either side of the equilibrium point.

To realise a continuous controller that stabilizes the system, one may design a sliding mode controller, where the sliding surface is:

$$s = \left(\frac{d}{dt} + K\right) \int_0^t e d\tau \tag{22}$$

where $e = \lambda - \lambda_d$. Therefore, $\dot{s} = \dot{e} + Ke$ and thus

$$\dot{s} = -\frac{\beta}{\omega_{dr}} \mu\left(\lambda\left(t\right)\right) + \frac{A}{\omega_{dr}} M_{br} + Ke \tag{23}$$

To stay on the surface $\dot{s} = 0$ is required. Solving for M_{br} and adding the term which forces the trajectory to stay on the surface we get the control input

$$M_{br} = \left(-Ke\omega_{dr} + \beta\mu\left(\lambda\left(t\right)\right)\right)/A \tag{24}$$

The control input is a function of the friction which is unknown. To overcome this an observer can be designed. However, it is known that friction observers have poor performance, and therefore it would be advisable to pursue a modified strategy. A heterogeneous hybrid controller may subsequently be implemented, which has a similar structure to the sliding mode controller. The controller uses 2 different control strategies. The first is active for λ smaller than 0.1 and aims to increase λ

$$M_{br} = -Ke\omega_{dr}/A \tag{25}$$

The proportional integral controller is subsequently used to stabilise the system around the equilibrium point $\lambda = 0.1$. The transfer function of the controller may be expressed as:

$$C\left(s\right) = K_p\left(1 + \frac{1}{sT_i}\right) \tag{26}$$

which implies that:

$$M_{br}\left(s\right) = -K_p\left(1 + \frac{K_i}{s}\right) e\left(s\right) \tag{27}$$

Due to the fact that the time span over which the dynamics of the system reside in the region of slip less than 0.1 is small, the gain for the proportional controller in the two regions is considered to be the same, i.e., K = K_p.

For plants that can be approximated by a first order dynamical system, the Ziegler-Nichols method for tuning PID controllers is recommended. In this case the closed-loop system step response is characterized by a damping ratio close to 0.5. The Ziegler-Nichols method is based on a stability analysis. The tuning of a PID controller is possible without knowledge of the plant and hence the method is well suited to tuning of controllers of stable plants with bounded uncertainties in the system parameters. For the closed loop system with the proportional gain set to some value and the integral gain set to zero, the proportional gain is increased until the system becomes oscillatory. Once the marginally stable response is obtained, all of the information necessary to calculate usable controller tuning constants is available. The oscillation frequency is denoted by m and the corresponding gain of the proportional controller by K_m. Subsequently, the optimal gains for the controller are given by

$$K_p = 0.45K_m \quad T_i = \frac{10\pi^2}{3\omega_m^2} \tag{28}$$

and hence

$$K_i = \frac{0.135K_m\omega_m^2}{\pi^2} \tag{29}$$

With reference to the presented method, the gains for a number of arbitrary driving wheel rotational speeds were obtained, using the single-input-single-output model indicated in figure 5 implemented in Simulink, in order to ascertain the correct scheduling of the gain with respect to ω_{dr}. The results are presented in Table 1. From

Table 1. Controller gains using Ziegler-Nichols method.

ω_{dr}	K_m	ω_m	K_p	K_i
10	20	9.5	9	24.7
100	200	9.56	90	250

the above analysis it may be seen that that the gain in the integral and the proportional element is approximately linear with respect to the driving wheel angular velocity. It is therefore proposed that the structure of the controller gain scheduling is

$$u(t) = k_p(\lambda_0(t) - \lambda(t))\omega_{dr}(t) + \int k_i(\lambda_0(t) - \lambda(t))\omega_{dr}(t) \quad (30)$$

This allows for a single value of a nominal gain to be selected based on the region of slip in which the system is operating as identified by k_i in the above equation

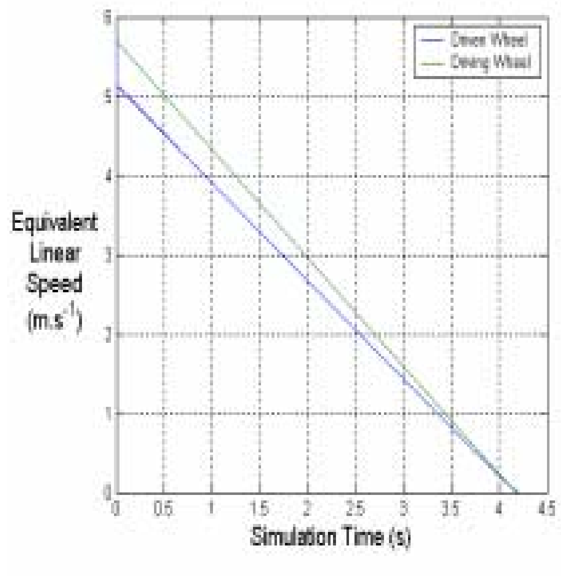

Fig. 6. Speed response of the ABS controller

4. SIMULATION

For the purpose of simulation of the system with the calculated gains, the full multiple-input-multiple-output mathematical model of the plant and controller was analysed in Simulink. The simulation was performed to determine the degree to which the system operation correlates with the required performance specification. The response of the system in decelerating the driving wheel may be plotted as the equivalent linear speeds of the driven and driving wheels against time. The result is shown in Fig. 6. From an analysis of Fig. 6 and Fig. 7 it may be seen that the controller accurately tracks the required setpoint of slip of 0.1. This is due to the fact that with the initial proportional controller active, for the region of slip less than 0.1, the state of the system is rapidly accelerated to the required region of operation and then the activation of the integral element maintains the state at the required setpoint.

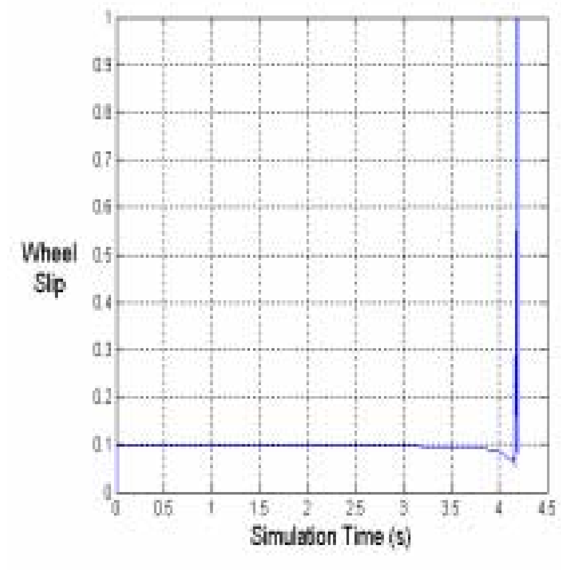

Fig. 7. Slip response of the ABS controller

5. CONCLUSIONS

Following a brief introduction to ABS, a non-linear car model was introduced which captured the longitudinal braking dynamics. In addition, a description of the mechanical controller test bed was given. It was shown that the dynamics of the quarter car test rig could be cast into a linear hybrid system with uncertainty. The uncertainties captured the unpredictable changes in road friction due to changes in surface conditions (wet, dry). It was shown that the dynamics are stable and that the maximum braking performance occurs at $\lambda = 0.1$. The control input space was computed and it was shown that for $\lambda \in [0{:}0.1]$ the slip has to be increased in order to increase the friction. For slip $\lambda > 0.1$, the slip has to be reduced to increase the friction and maintain steerability. It was shown that a PI controller with gains scheduled in relation to the driving wheel rotational speed and the measured slip could be used to stabilize the system about the optimum slip $\lambda = 0.1$. The analysis did not take into account the controller time lag or the actuator dynamics, and hence further work could concentrate on increased accuracy in the representation of the full system dynamics.

REFERENCES

Buckholtz, K. R. (2002). Reference input wheel slip tracking using sliding mode control. In: *Proceedings of SAE 2002 World Congress*. number 2002-01-0301. Detroit.

Drakunov, S., Ü. Özgüner, P. Dix and B. Ashrafi (1995). ABS control using optimum search via sliding modes. *IEEE Transactions on Control Systems Technology* **3**(1), 79–85.

Jiang, F. and Z. Gao (2001). An application of nonlinear PID control to a class of truck ABS problems. In: *Proceedings of IEEE Conference on Decision and Control*.

Johansen, T. A., I. Petersen, J Kalkkuhl and J. Lüdemann (2001). Hybrid control strategies in ABS. In: *Proceedings of American Control Conference*. Arlington.

Johansen, T. A., I. Petersen, J Kalkkuhl and J. Lüdemann (2003). Gain-scheduled wheel slip in automotive brake systems. *IEEE Transactions on Control Systems Technology* **11**, 1–20.

Jun, C. (1998). The study of ABS control system with different control methods. In: *Proceedings of the 4^{th} International Symposium on Advanced Vehicle Control*. number 9837373. Nagoya, Japan.

Petersen, I., T. A. Johansen, J. Kalkkuhl and J. Lüdemann (2003). Wheel slip control using gain-scheduled LQ-LPV/LMI analysis and experimental results. In: *Proceedings of European Control Conference*. Cambridge.

Schinkel, M. (n.d.). Control of Antilock Brake with Hybrid Heterogeneous Controller, *Nondetermenistic Hybrid Dynamical Systems*. PhD thesis.

Solyom, S. (2002). Synthesis of a model-based tire slip controller. PhD thesis. Department of Automatic Control, Lund Institute of Technology, Lund, Sweden.

Wellstead, P. E. and N. B. O. L. Pettit (1997). Analysis and redesign of an antilock brake system controller. *IEE Proceedings on Control Theory and Applications* **144**(5), 413–426.

Will, A. B., S. Hui and S. H. Żak (1998). Sliding mode wheel slip controller for an antilock braking system. *International Journal of Vehicle Design* **19**(4), 523–539.